Full Paper

Wiley Online Library

ELECTROANALYSIS

DOI: 10.1002/elan.202060331

Comparative Study of a Sensing Platform via Functionalized Calix[4]resorcinarene Ionophores on QCM Resonator as Sensing Materials for Detection of Heavy Metal Ions in Aqueous Environments

Abdul Shaban*[a] and Larbi Eddaif[a, b]

Abstract: A flow type quartz crystal microbalance with impedance analysis capability (QCM-I) chemical sensor was tested for heavy metal (HM) ions detection in aqueous solutions. The sensor development is based upon the complexing ability of the functionalized AT-cut quartz resonator gold surface, by calixresorcinarenes, towards the HM ions. These calixresorcinarenes coated QCM sensors were tested for selectively adsorbing HM ions, such as copper, lead, mercury, and cadmium, from solution over a wide range of concentration (5-1000 ppm) through complexation with functional groups in the coating layers. QCM-Calix based chemosensors, C-dec-9-en-1-ylcalix[4]resorcinarene (ionophore I), C-undecylcalix[4] resorcinarene (ionophore II), C-dec-9-enylcalix[4]resorcinarene-O-(S-)-α-methylbenzylamine (ionophore III) and C-dec-9-enylcalix[4]resorcinarene-O-(R +)-α-methylbenzylamine (ionophore IV), were synthesized and immobilized to detect HM ions of Pb^{2+}, Cd^{2+}, Hg^{2+}, and Cu^{2+} in aqueous solutions. Using the impedance analysis, which facilitates a complete description of the acoustic loading of the crystal surface, the full width at half maximum of the QCM resonance peak (FWHM) values are obtained from the impedance spectra. FWHM variations revealed the effectiveness of the proposed ionophores in detecting HM at different levels. Sensitivities and wide linear relationships between HM concentration and FWHM were interpreted. Detection limits of (0.32, 0.57, 0.37, 0.89 ppm) and (1.63, 0.18, 0.76, 0.2 ppm) were determined for ionophore I and II, for Cd^{2+}, Cu^{2+}, Hg^{2+} and Pb^{2+} ions, respectively. Ionophore (I) showed binding preferences towards Cd^{2+} ions where ionophore (II) produced similar selectivity toward Cu^{2+} and Pb^{2+} ions. Ionophores III and IV were used for the assessment of △FWHM values to comprehend the detection affinities of the ionophores toward HM ions.

Keywords: Calixresorcinarenes · chemosensors · heavy metals · piezogravimetric sensor

1 Introduction

The term ''heavy metal'' (HM) refers to any metal and metalloid element with a rather high density (3.5 to 7 g. cm^{-3}) and high toxicity even at low concentrations [1]. That includes several common metals such as mercury (Hg), cadmium (Cd), copper (Cu), and lead (Pb). Heavy metals diverge extensively in their chemical properties and applications and thus can pollute the nearby aquatic bodies of water through several activities. Recently, owing to the change of the environmental regulations, more attention is dedicated to the HM ions levels detection procedures in food, pharmaceutical, industrial and environmental research [1,2].

Conventional techniques to analyze metals ions include cold vapor atomic absorption spectrometry, inductively coupled plasma mass spectrometry, UV visible spectrophotometry, and X-ray absorption spectroscopy. These techniques, even though are extremely precise, suffer from the shortcomings of being uneconomical, time-consuming, complicated operations that require qualified personnel, and immobility (i.e. mostly laboratory bound) [3–5].

Recently, the applications of chemical sensors as an alternative approach to conventional analytical procedures to quantify trace amounts of toxic HM have found great consideration. Innovative ionophores-based chemical sensors proved to be a suitable alternative that possesses several advantages [6–8]. Ionophores are a class of compounds that formulate complexes with specific HM

[a] A. Shaban, L. Eddaif
Functional Interfaces Research Group, Institute of Materials and Environmental Chemistry, Research Centre for Natural Sciences, Bp., Hungary
E-mail: shaban.abdul@ttk.hu
[b] L. Eddaif
Doctoral School of Material Sciences and Technologies, Óbuda University, Faculty of Light Industry and Environmental Engineering, Bp., Hungary.

ions and facilitate their adsorption on the detecting platform. Typically, an ionophore has a hydrophilic pocket (or hole) that forms a binding site specific for a particular ion [9].

A unique feature of Ionophore-based sensors (IBS) is offering data about free ion concentration, which is greatly appropriate and essential in environmental monitoring. Recently, comprehensive investigations in the area of IBS led to enormous improvements in the analytical performance of such sensors [10,11]. Innovative transduction mechanisms are continuously being discovered and many novel sensing materials are being synthesized.

Macrocyclic ionophores as cyclodextrines [12,13], crown ethers [14], and calixarenes/ calixresorcinarenes [2,10,11,15–19] are effectively employed as surface modifiers and selective sensing platforms. Calix-ionophores, due to their distinctive host-guest interactions, selective capabilities, and amphiphilic character are broadly used in sensing networks [17,20–24].

Environmental monitoring chemosensors, based on the use of piezoelectric technique, are among the most frequently used [10,25]. Among the piezoelectric methods, the quartz crystal microbalance (QCM) has been extensively explored as a transducer for HM monitoring in gaseous and aqueous media. In modern QCM technologies, resonance frequencies and dissipations are generally measured by either of two types of readout procedures [26]: by the impulse excitation method with the measurement of the decay of crystal's oscillation after turning off the excitation, (QCM-D, Q-Sense, Sweden); or by impedance analysis by means of a network analyzer that measures the frequency spectrum of the impedance (QCM-I, MicroVacuum Ltd, Hungary).

Through the impedance analysis procedure, the sensor's complex impedance over a series of frequencies around fundamental and odd overtone resonance frequencies (impedance or conductance vs. frequency) are recorded and curves are fitted by measuring software to accurately determine the resonance frequency (frequency of the conductance maximum, f_r) and the bandwidth of the peak (full width at half maximum, FWHM), both can alter in response to the sensor surface variations [25,26]. The FWHM is linked to the dissipation (D) determined by QCM-D (Via "ring-down" method) and is inversely proportional to the quality factor (Q) of the crystal:

$$\mathrm{FWHM}_n/f_n = \mathrm{D} = 1/\mathrm{Q} \quad (1)$$

Normalization of the △FWHM alteration is determined by dividing the change in the measured values by the used overtone (n).

The objective purpose of this investigation is to put forward and realize a Calix-QCM sensor based on synthesized macrocyclic ionophores. Subsequently, the fabricated Calix-QCM sensor is examined by detecting the liquid load on the surface of the oscillating crystal and applying the impedance analysis to investigate and compare the effectiveness in Pb^{2+}, Cd^{2+}, Hg^{2+}, and Cu^{2+} ions detection. The sensitivity, limits of detection, and selectivity related characteristics were calculated. The applied ionophore platforms were: C-dec-9-en-1-ylcalix[4]resorcinarene (ionophore I), C-undecylcalix[4]resorcinarene (ionophore II), C-dec-9-enylcalix[4]resorcinarene-O-(S-)-α-methylbenzylamine (ionophores III) and C-dec-9-enylcalix[4]resorcinarene-O-(R+)-α-methylbenzylamine (ionophores IV). The properties of the functional groups attached to the basic skeleton of resorcinarenes beside the structure results in the interaction with the cations of the heavy metals. These characteristics of resorcinarenes permit their employment in the development of ion-selective potentiometric sensors [27].

2 Experimental

2.1 Synthesis and Characterization of Ionophores

Four calix[4]resorcinarene derivatives, were synthesized based on simple condensation reactions, as ionophores, I, II, III, VI, and their chemical structures are displayed in Figure 1. Furthermore, the ionophores chemical and structural characterization by FTIR, NMR, XRD, and TG-DSC-MS was performed as described earlier [28].

2.2 Materials and Methods

All applied aqueous solutions were prepared by analytical grade chemicals and with deionized Milli-Q water (18 MΩcm). Concentrations of 5, 25, 250, 500, and 1000 ppm of Pb^{2+}, Cu^{2+}, Hg^{2+}, and Cd^{2+} ions were prepared from Lead(II) Nitrate ($Pb(NO_3)_2$), Copper(II) Nitrate ($Cu(NO_3)_2$), Mercury(II) Chloride ($HgCl_2$) and Cadmium(II) Nitrate ($Cd(NO_3)_2$), respectively. The applied apparatus for the impedance analysis is a QCM-I-008 system (MicroVacuum Ltd). The system has the following characteristics: standard resonance frequency sensitivity $\sim 2\times10^{-1}$ Hz, standard dissipation sensitivity $\sim 1x10^{-7}$ and mass sensitivity ≤ 1 ng.cm^{-2}, in liquid media [29].

The sensor quartz crystal (QC) was a 5 MHz, AT-cut, 14 mm diameter type with up to the 13th overtone for a 1–80 MHz frequency range. Overtones, (1st (fundamental), 3rd, 5th, and 7th), representing frequencies of 5, 15, 25, 35 MHz, respectively, were applied during the experiments. The volume of flow-cell is ~40 µl and the temperature is automatically thermostated at 25 °C. BioSense software performed full control of the QCM-I instrument. Two measurement modes were performed: measurement of resonance curve (Resonance) and calculation of the resonance frequency & FWHM up to 80 MHz and continuous measurement of resonance parameters (QCM-t). The impedance analysis is performed at each test time for each overtone, as well the *in-situ* data offers the basis of measurements of calculations on the interface film surface mass density and its viscoelastic characteristics as well.

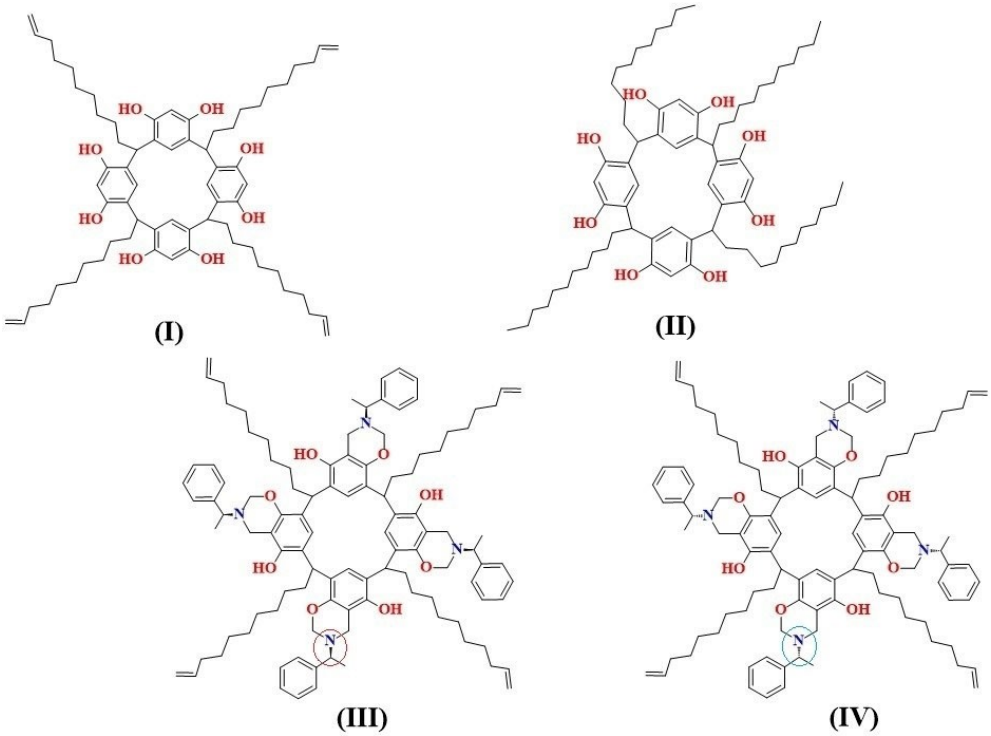

Fig. 1. Molecular structures of ionophores (I, II, III and IV).

2.3 Modification of the Sensor Surfaces by Ionophores

Ionophores immobilization on QC is achieved through physical adsorption, where the ionophores molecules are detained on the Au surface by physical forces, such as hydrophobic interactions. Physical immobilization is preferred for its simplicity and applicability.

The gold surface of the sensor chip was soaked in acetone (10 min), in washing solution (ammonia (NH_3 (30 %)), hydrogen peroxide (H_2O_2 (30 %)) and Milli-Q water (1 : 1 : 5 volume ratio)), at 70 °C (10 min), then rinsed by Milli-Q water and allowed to dry.

The ionophores-based coatings were prepared by dissolving an appropriate amount of ionophore (2 mg) in 1 mL of chloroform (99.99 %, stabilized with 1 % EtOH). The film immobilization was performed by drop-casting 10 µL of the dissolved ionophore solution on the previously cleaned QC Au surface and then let the solvent evaporate at room temperature in a desiccator.

3 Results and Discussion

The detection ability of the applied calix[4]resorcinarene ionophores (I, II, III, IV) is observed against HM ions (Pb^{2+}, Cu^{2+}, Hg^{2+}, and Cd^{2+}) in aqueous solutions via *In-situ* QCM-I measurements with an advanced instantaneous layer characterization parameter (FWHM).

3.1 Interaction of Ionophores with Au-Surface

Generally, resorcinarenes are capable to perform as host molecules due to the existence of cavities. Ionophores binding with the sensor's surface is due to electronic interactions (Charge transfer) [30,31], usually between ligands free electrons and Au surface, generating distinct sensing platforms capable of capturing toxic HM. Thermodynamic stability of the Au surface is well documented [32,33], but high reactivity of free/mobile electrons makes it easy to form either O–Au bonds (via ionophores' hydroxyl groups) and/or Au-Aromatic cycles (via aromatic π electrons). Insertion of O atoms through the Au surface creates higher electronic density favoring well-defined buildup.

3.2 Impedance Analysis Results

Detection capacities of the studied ionophores towards Cd^{2+}, Cu^{2+}, Pb^{2+}, and Hg^{2+} in aqueous solutions were obtained through the application of *in-situ* QCM-I, with the objective of identifying the most effective sensing platform in terms of detection characteristics: FWHM variations, sensitivity and selectivity, linear ranges, and detection limits and quantification. For the impedance analysis, the procedure to obtain data of typical normalized values of △FWHM in time is explained in details previously [34].

3.2.1 Calibration of the Uncoated QCM Resonator

The purpose of this simple experiment is to demonstrate that there is no interaction between the HM cations and the Au crystal surface. The results can be applied to show the stability of the apparatus during the detection measurement. The QC normalized △FWHM variation as a result of the injection of HM cations (Cd^{2+}, Hg^{2+}, Cu^{2+}, and Pb^{2+}), at different concentrations on bare Au surface was shown [34]. The results confirm that the addition of the cations had no effect on the △FWHM of the resonator's gold surface therefore it indicates that neither chemical nor physical interaction between the cations and the gold surface occurred. Nevertheless, the apparent insignificant fluctuations in the plots are generally owed to the wetting of the dry sensor's surface after the direct contact with the aqueous injection. Therefore, employing sensing networks is compulsory to increase the resonator's sensitivity.

3.2.2 Detection of HM Ions by Ionophores-Coated QCM Sensor

Normalized values of △FWHM shifts for ionophores (I, II) against all applied HM ions at all concentrations are listed in Table 1. Those values were extracted from the endpoints of ΔFWHM plots. As shown in Table 1, a trend that the ΔFWHM shifts are a concentration-dependent, i.e. varies by increasing HM ions concentrations, displaying the ability of the Calix-QCM based platforms to monitor the HM ions detection. Values of ΔFWHM variations associated to ionophores III and IV are denoted for comparison purposes and are reported previously [34].

3.2.3 Detection Limit and Quantitation for the Ionophores

Detection features manifesting in low limits of detection (LODs), high sensitivities and selectivity, are compulsory for sensors practical applications. Figure 2 and Table 2

Table 1. Normalized ΔFWHM variations for ionophores **I** and **II** at various (Cd^{2+}, Cu^{2+}, Pb^{2+}, and Hg^{2+}) concentrations.

HM	C_{HM} (ppm)	ΔFWHM (Hz) *Ionophores*	
		I	*II*
	0	0.08 ± 0.02	0.44 ± 0.05
	5	7.70 ± 0.01	4.47 ± 0.03
Cd^{2+}	25	19.31 ± 0.04	9.54 ± 0.04
	250	38.04 ± 0.30	11.31 ± 0.01
	500	97.45 ± 1.20	21.17 ± 0.20
	1000	202.70 ± 2.40	27.49 ± 0.02
	0	0.67 ± 0.01	0.18 ± 0.03
	5	14.59 ± 0.02	2.70 ± 0.01
Cu^{2+}	25	16.62 ± 0.04	3.72 ± 0.04
	250	28.51 ± 0.03	9.55 ± 0.05
	500	42.14 ± 0.20	45.93 ± 0.08
	1000	64.89 ± 0.09	52.26 ± 0.07
	0	0.56 ± 0.06	0.00 ± 0.00
	5	5.49 ± 0.02	10.04 ± 0.01
Hg^{2+}	25	6.05 ± 0.01	11.81 ± 0.02
	250	25.19 ± 0.07	21.17 ± 0.04
	500	51.24 ± 0.03	23.96 ± 0.03
	1000	59.59 ± 0.04	82.09 ± 0.12
	0	0.21 ± 0.03	0.00 ± 0.00
Pb^{2+}	5	4.20 ± 0.01	15.34 ± 0.01
	25	6.65 ± 0.02	18.13 ± 0.03
	250	21.49 ± 0.05	26.22 ± 0.04
	500	31.67 ± 0.04	44.92 ± 0.08
	1000	32.77 ± 0.07	59.33 ± 0.12

Table 2. Sensing characteristics of ionophores **I** and **II** based chemosensors.

	Ionophore I				*Ionophore II*			
HM	LR ppm	Sensitivity Hz.ppm^{-1}	LOD ppm	LOQ ppm	LR ppm	Sensitivity Hz.ppm^{-1}	LOD ppm	LOQ ppm
Cd^{2+}	250–1000	0.225	0.32	0.96	5-1000	0.021	1.63	4.90
Cu^{2+}	2–1000	0.052	0.57	1.71	1-250	0.028	0.18	0.54
Hg^{2+}	1–500	0.093	0.37	1.11	3-500	0.030	0.76	2.28
Pb^{2+}	3–500	0.057	0.89	2.67	1-1000	0.048	0.20	0.60

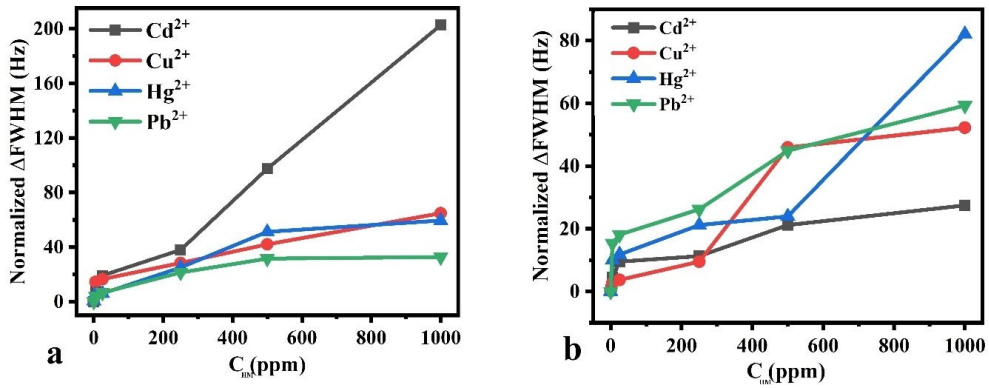

Fig. 2. Dynamic ranges of ionophores I (**a**) and II (**b**).

exhibit the sensing characteristics for the tested ionophores (dynamic and linear ranges, sensitivities, LOD and LOQ values), regarding Cd^{2+}, Hg^{2+}, Pb^{2+}, and Cu^{2+} ions. Sensitivities of the ionophores, expressed in (Hz/ppm), are the slopes of the linear regression applied to the calibration curves, while LODs are calculated using eq. (2):

$$LOD = 3\sigma/S \quad (2)$$

where σ is the fitted curves' standard deviation and *S* is the sensor's sensitivity.

The detection limits (LOD) and LOQ values of the QCM sensor coated with ionophore I and II for HM ions detection are listed in Table 2. By evaluating the calibration curves and detection data (Figure 2 and Table 2), it is evident that ionophore (I) showed more selectivity to Cd^{2+} ions (Sensitivity = 0.225 Hz/ppm and LOD = 0.32 ppm), whereas ionophore (II) performed similarly selective to Cu^{2+} and Pb^{2+} with sensitivities = 0.028 and 0.048 ppm/Hz and LODs = 0.18 and 0.20 ppm, respectively. Wide linear ranges, high sensitivities, and low LODs were attained for all studied cases. The detection limits were obtained: LODs of 0.32, 0.57, 0.37, 0.89 ppm (ionophore I), 1.63, 0.18, 0.76, 0.2 ppm (Ionophore II) for the Cd^{2+}, Cu^{2+}, Hg^{2+}, and Pb^{2+} ions, respectively.

3.2.4 Affinity of Ionophores Platforms Toward HM Cations

Figures 3–6 present a radar form of the △FHWM values of QCM-I sensors coated with ionophores (I), (II), (III), and (IV) for the affinity toward Pb^{2+}, Hg^{2+}, Cd^{2+}, and Cu^{2+} in aqueous solution. This approach is advantageous to understand the sensing performance of calix[4]-coated QCM sensors towards different HM ions in aqueous solution. Ionophores I and II are part of the present work, and III and IV are from the previous investigation [34]. The variations in △FWHM are presented for each HM ion (Cd^{2+}, Hg^{2+}, Pb^{2+}, and Cu^{2+}), at each concentration (5, 25, 250, 500, and 1000 ppm), and combining the response of the four calixresorcinarenes at the same time.

The radar plot of the △FWHM variations of ionophores I, II, III, and IV in the detection of Cd^{2+} cations at different concentrations (5, 25, 250, 500, and 1000) is displayed in Figure 3. It is notable that ionophore I showed the highest detection sensitivity at all tested concentrations while ionophore II was effective at lower concentrations (5 and 25 ppm). As the concentration of cations increased the sensitivity of ionophore II decreased slightly. Ionophore III produced low sensitivity at all concentrations while ionophore IV showed slight improvement of sensitivity at high cations concentrations (500 and 1000 ppm).

Figure 4 is associated with the detection of Cu^{2+} ions by ionophores I, II, III, and IV at different concentrations (5, 25, 250, 500, and 1000). It revealed that again ionophore I produced the best detection sensitivity all over the concentration range and the detection increased by increasing the Cu^{2+} concentration. Ionophore II showed good detection at concentrations above 500 ppm while low detection at lower concentrations. Ionophore III showed a slight increase at 1000 ppm while ionophore IV had low detection all over the concentration range.

The detection sensitivity toward Hg^{2+} ions is illustrated in the radar plot in Figure 5. Ionophore II displayed the highest detection sensitivity at all tested concentrations while ionophore I had high detection at concentrations above 250 ppm. Ionophore III and IV displayed moderate detection at lower concentration values.

The case of Pb^{2+} ions detection by the ionophores I, II, III, and IV is depicted in Figure 6. Similar to the case of Hg^{2+}, ionophore II once again is the most sensitive toward all tested concentrations, while ionophore I was more effective as the ions concentration was increased. Ionophores III and IV had moderate and low detections, respectively.

From the above observations, it is clear that the proposed approach is recommended to comprehend the sensing behavior and affinities of different oligomers towards HM ions in aqueous solutions. When comparing responses of the studied potential sensors, it's revealed that Ionophores III and IV had moderate detection ability

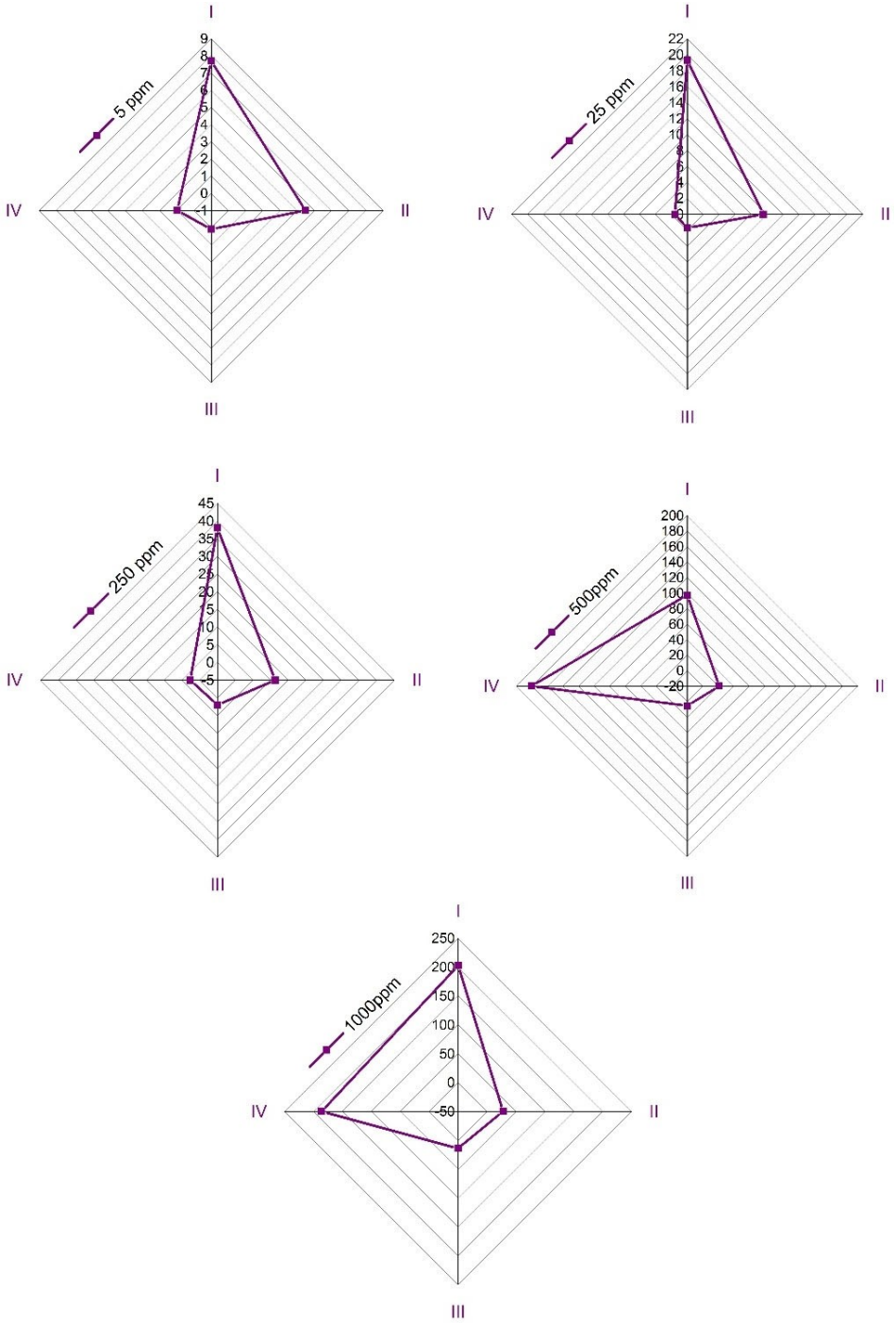

Fig. 3. FWHM variations of calix-QCM chemosensors for several Cd^{2+} concentrations

towards all HM ions with selective preferences, though compounds I and II had significantly powerful interactions and high binding affinities. The sensor system, using Ionophore I coating material, demonstrated the best sensitivity of detection of Cd^{2+} and Cu^{2+} ions, however, ionophore II was more selective towards Hg^{2+} and Pb^{2+} ions.

3.2.5 Correlation between Ionophores Molecular Structures and Affinity Towards HM

The selective recognition and/or detection of HM cations by resorcinarenes, are acceptable if certain parameters are satisfied such as: there must be a significant complementarity between the ionophores cavities dimensions and the guest ions e.g. HM. The substituents and the number of donor sites present in the host molecular

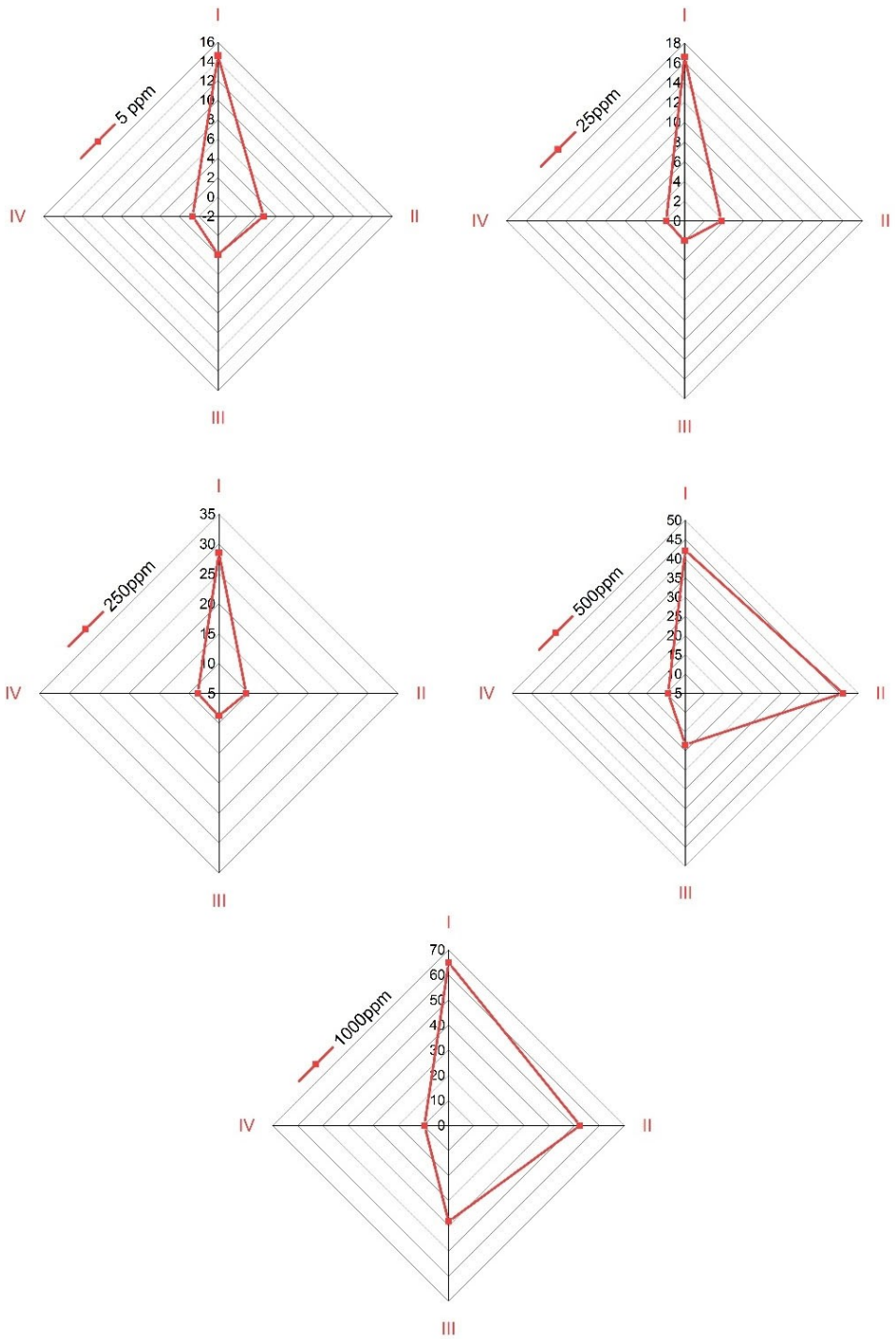

Fig. 4. FWHM variations of calix-QCM chemosensors for different Cu^{2+} concentrations

structure, also have a great influence on its complexing properties.

These facts are translated in our investigation, by selective binding of ionophore (I) with cadmium and copper ions ($r(Cu^{2+}) = 0.73$ Å $< r(Cd^{2+}) = 0.95$ Å), and of ionophore (II) with mercury and lead ions ($r(Hg^{2+}) = 1.02$ Å $< r(Pb^{2+}) = 1.19$ Å), which from one point of view, confirms that a cone conformation may be adopted by these molecules, helping the HM entrapment, and contrarily that relatively light HM (Cu^{2+} and Cd^{2+}) are privileged to complex with ionophore (I) over ionophore (II).

The enantiomeric carriers ionophore (III) and ionophore (IV) showed detection capability towards all tested HMs, but were not as selective compared to ionophores (I) and (II). A simple explanation based on

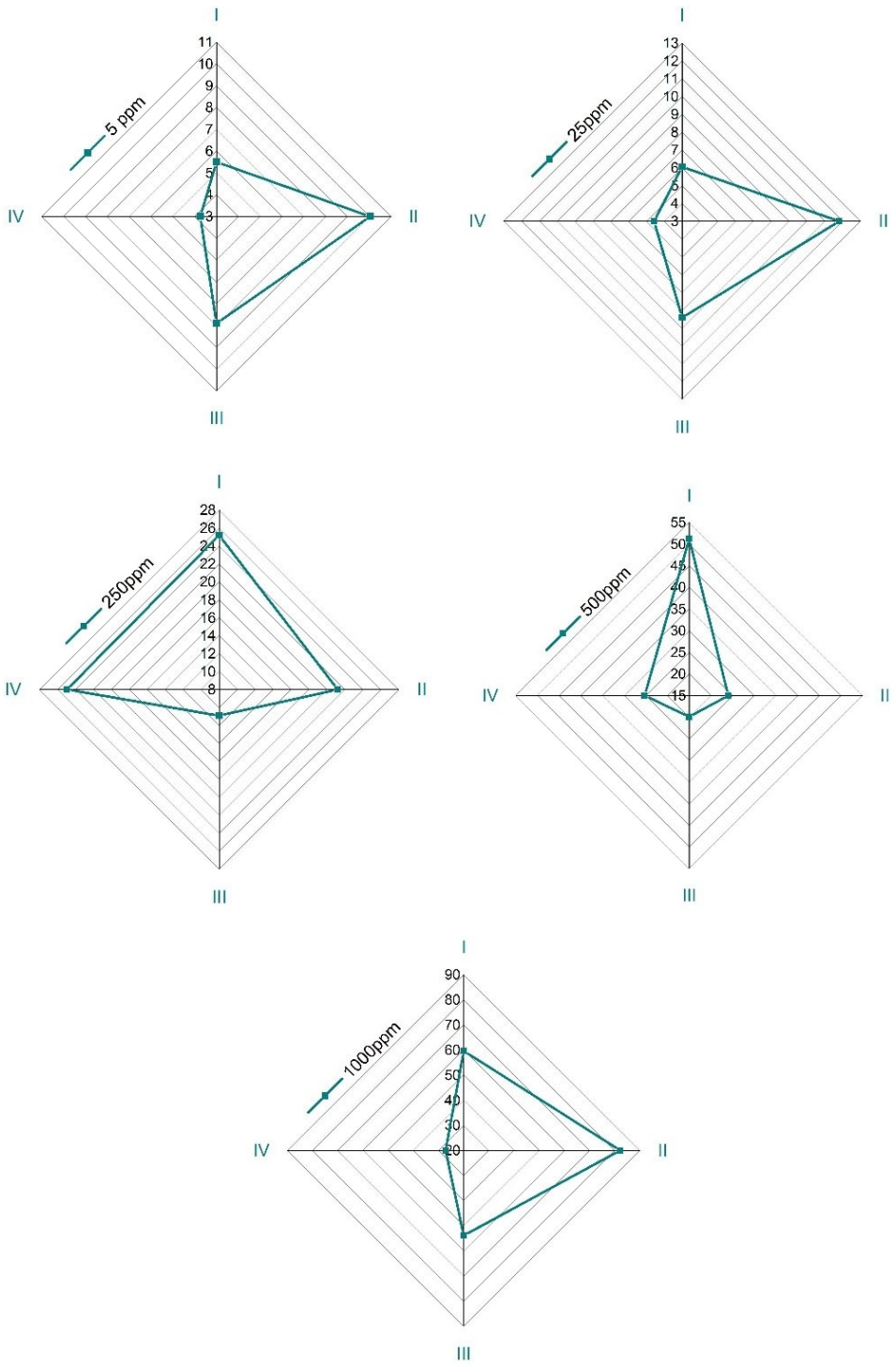

Fig. 5. FWHM variations of calix-QCM chemosensors for various Hg^{2+} amounts

their molecular structures, or adopted conformations, is probably the cause. As well, their large molecular groupings cause steric effects (steric hindrance), this latter is normally not enough to stop a complexation reaction, but may slow it down or change the reaction mechanism (as it's the case herein).

3.3 Hypothetical Mechanism of HM Detection

The detection mechanism of HM ions is strongly dependent on the interactions of host-guest complexation between HM and already attached ligands on the QCR gold surface [35–39]. Calix oligomers are having heteroatoms as O, electron transfer between ionophores and

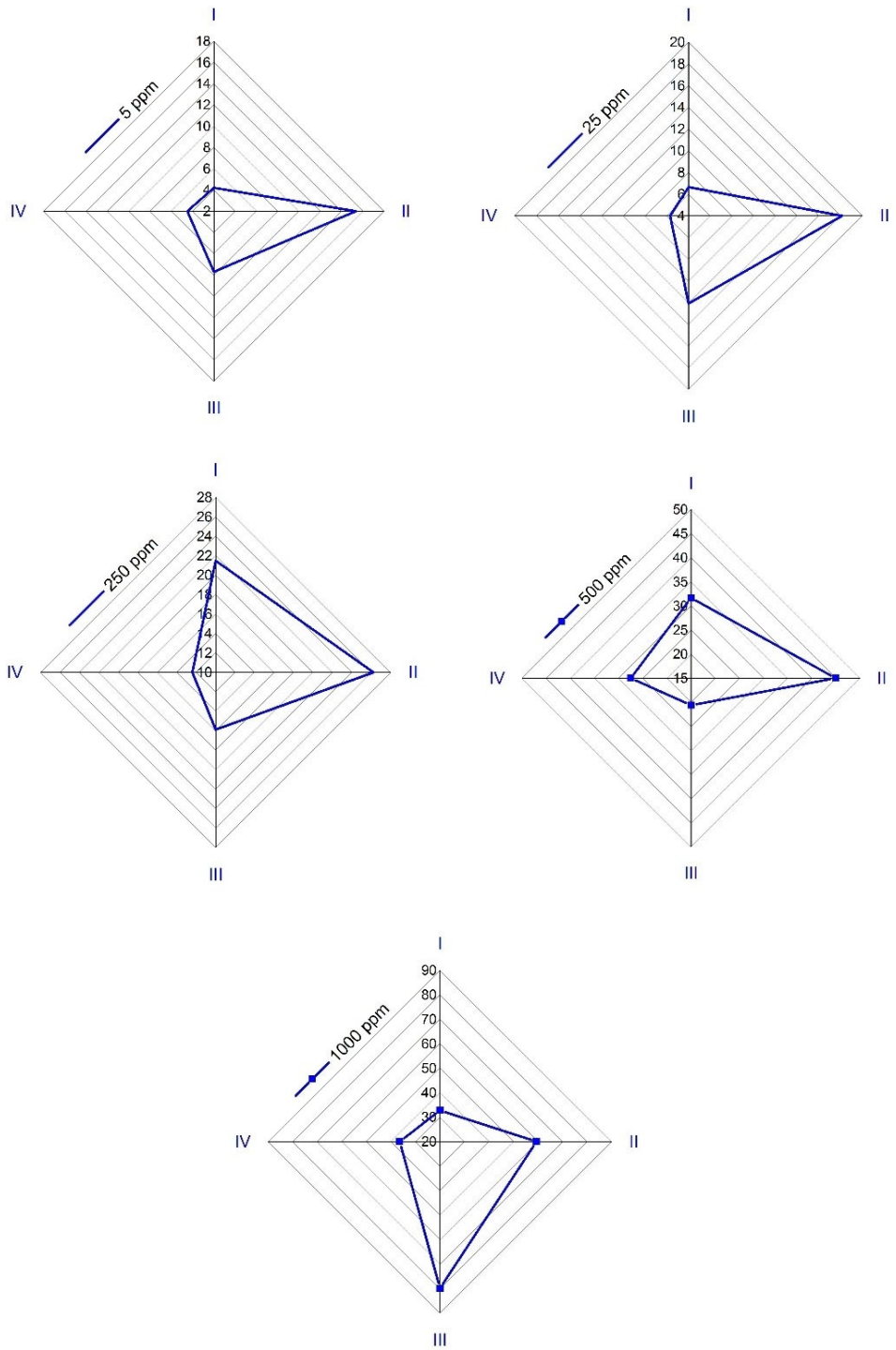

Fig. 6. FWHM shifts of calix-QCM chemosensors for various Pb^{2+} amounts

HM is therefore supported. In consideration of this process, HM accumulation at the gold surface-electrolyte interface is induced, the ions buildup is detected piezo-gravimetrically. Considering the chelation fact of HM ions and ionophores [40], complexes may be formed on the Au surface as described by eq. (3):

$$(\text{Ligand})_{surface} + (HM^{n+})_{solution} \rightarrow [HM^{n+}\text{Ligand}]_{surface} \quad (3)$$

where HM^{n+} stands for (Cd^{2+}, Cu^{2+}, Pb^{2+}, and Hg^{2+}), Ligand = Ionophores I, II, III, and IV).

Accumulated HM at the Au surface can fit within ionophores' cavities (adsorption), either via π electrons of aromatic cycles (cation-π bonds) and/or oxygen electron-free doublets. This kind of solid interactions is of immense

importance in terms of ion-binding potential between ligands and HM ions. The intention is to examine whether HM would be bound to the calixresorcinarenes when immobilized on gold transducer through by the conversion of an acoustic signal into FWHM variations [41].

Such HM-Ionophores bonds, however, are rigid enough and cannot be easily broken by distilled water regenerating solution (RS) to desorb HM eq. (4), as it's time limitation. The development of an appropriate regeneration method is of huge interest in our ongoing research.

$$(HM^{n+})_{solution+\ surface} + (RS)_{solution} \rightarrow [HM^{n+}RS]_{solution} \quad (4)$$

It is obvious that as mentioned in the literature, the arbitrary ordering of the ionophore molecules on the QCR gold surfaces has a significant effect on sensing efficiency. For that reason, it is deliberated that other coating methods, specifically Langmuir-Blodgett and spin coating, are more suitable to obtain well-ordered, homogeneous, and stable Calix layers on the gold surfaces [42]. Figure 7 displays a not-in-scale cross-section of the electrode-solution interface showing the attachment of the ionophores ((I), (II), (III), and (IV) on the QC gold surface and the HM-resorcinarenes interactions.

4 Conclusions

In conclusion, the sensing studies of Calix-QCM sensors coated by some resorcinarene derivatives (ionophores I, II, III, and IV) bearing different functional groups for some selected HM ions (Cd^{2+}, Cu^{2+}, Pb^{2+}, and Hg^{2+}), were effectively accomplished via *in-situ* QCM-I.

Initial experiments showed that all Calix-QCM sensors showed different detection sensitivities toward different HM ions. The radar plots of the FWHM changes (Impedance analysis), demonstrated that Calix-QCM sensor coated with ionophores (I) and (II) were the most useful sensor for HM ions with the following of detection limits: LODs of 0.32, 0.57, 0.37, 0.89 ppm (ionophore I), 1.63, 0.18, 0.76, 0.2 ppm (ionophore II) for the Cd^{2+}, Cu^{2+}, Hg^{2+}, and Pb^{2+} ions, respectively.

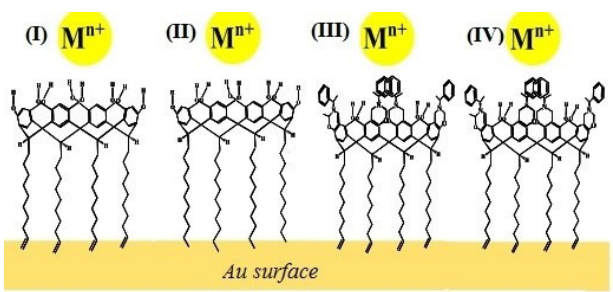

Fig. 7. Not-in-scale cross-section of the electrode-solution interface showing the attachment of the ionophores (I–IV) on QC gold surface and the Au-resorcinarenes interactions.

Interacting preferences towards cadmium ions (LOD = 0.32 ppm, Sensitivity = 0.225 Hz/ppm) for ionophore I were revealed, equally towards copper and lead cations (LODs = 0.18 and 0.2 ppm. Sensitivities = 0.028 and 0.048 ppm/Hz) in case of ionophore II.

Illustrating the sensing affinities of different sensor platforms towards HM ions, ionophores III and IV were used for comparison reasons. Ionophore II was selective to mercury and lead, though ionophore I can be selected as the best coating material for the sensitive detection of cadmium and copper ions.

Acknowledgments

We appreciate the support from the [BIONANO_GINOP-2.3.2-15-216-00017] project. The funding from the Stipendium Hungaricum Scholarship program is appreciated. Many thanks to Szendrő István from MicroVacuum Ltd for loaning the QCM-I apparatus. The authors thank Prof. Telegdi Judit for useful consultations.

Data Availability Statement:

The data sets generated during and/or analyzed during the current study are not available due to: the research work is part of Ph. D. dissertation for Larbi Eddaif, which is not publicly defended yet but are available from the corresponding author on reasonable request.

References

[1] M. E. Morales, R. S. Derbes, C. M. Ade, J. C. Ortego, J. Stark, P. L. Deininger, A. M. Roy-Engel, *PLoS One* **2016**, *11*, 1–21.
[2] L. Eddaif, A. Shaban, J. Telegdi, *Int. J. Environ. Anal. Chem.* **2019**, *99*, 824–853.
[3] R. A. Mohamed, A. M. Abdel-Lateef, H. H. Mahmoud, A. I. Helal, *Chem. Speciation Bioavailability.* **2012**, *24*, 31–38.
[4] M. Batsala, B. Chandu, B. Sakala, S. Nama, S. Domatoti, *Int. J. Res. Pharma. Chem.* **2012**, *2*, 671–680.
[5] O. V. S. Raju, P. M. N. Prasad, V. Varalakshmi, Y. V. R. Reddy, *Int. J. Innov. Res. Sci. Eng. Technol.* **2014**, *3*, 9743–9749.
[6] X. Cai, J. Li, Z. Zhang, F. Yang, R. Dong, L. Chen, *ACS Appl. Mater. Interfaces.* **2014**, *6*, 305–313.
[7] L. Chen, X. Wang, W. Lu, X. Wu, J. Li, *Chem. Soc. Rev.* **2016**, *45*, 2137–2211.
[8] E. Singh, M. Meyyappan, H. S. Nalwa, *ACS Appl. Mater. Interfaces.* **2017**, *9*, 34544–34586.
[9] J. C. Freedman, Chapter 4 - Ionophores in Planar Lipid Bilayers, N. Sperelakis (Edt), in Cell Physiology Source Book (4th Ed.), Academic Press, 2012, 61–66, https://doi.org/10.1016/B978-0-12-387738-3.00004–4.
[10] D. W. Grainger, D. G. Castner, *Comprehensive Biomaterials II* **2017**, *3*, 1–24.
[11] G. N. M. Ferreira, *Trends Biotechnol.* **2009**, *27*, 689–697.
[12] A. U. Alam, M. M. R. Howlader, N.-X. Hu, M. J. Deen, *Sens. Actuators B* **2019**, *296*, 126632.
[13] D. Prochowicz, A. Kornowicz, J. Lewiński, *Chem. Rev.* **2017**, *117*, 13461–13501.

[14] H. M. Chawla, G. Hundal, S. Kumar, P. Singh, *J. Inclusion Phenom. Macrocyclic Chem.* **2012**, *72*, 323–330.
[15] L. Wang, X. Wang, G. Shi, C. Peng, Y. Ding, *Anal. Chem.* **2012**, *84*, 10560–10567.
[16] F. Cadogan, P. Kane, M. A. McKervey, D. Diamond, *Anal. Chem.* **1999**, *71*, 5544–5550.
[17] V. Arora, H. M. Chawla, S. P. Singh, *Arkivoc* **2007**, *2*, 172–200.
[18] P. Montmeat, F. Veignal, C. Methivier, C. M. Pradier, L. Hairault, *Appl. Surf. Sci.* **2014**, *292*, 137–141.
[19] S. Lee, K. Jang, C. Park, J. You, T. Kim, C. Im, J. Kang, H. Shin, C.-H. Choi, J. Park, S. Na, *New J. Chem.*, **2015**, *39*, 8028–8034.
[20] K. M. O'Connor, D. W. M. Arrigan, G. Svehla, *Electroanalysis.* **1995**, *7*, 205–215.
[21] E. Van Dienst, W. I. Bakker, J. F. Engbersen, W. Verboom, D. N. Reinhoudt, *Pure Appl. Chem.* **1993**, *65*, 387–392.
[22] D. Diamond, G. Svehla, E. M. Seward, M. A. McKervey, *Anal. Chim. Acta.* **1988**, *204*, 223–231.
[23] C. Bouvier-Capely, A. Manoury, A. Legrand, J. P. Bonthonneau, F. Cuenot, F. Rebiere, *J. Radioanal. Nucl. Chem.* **2009**, *282*, 611.
[24] R. Ebdelli, A. Rouis, R. Mlika, I. Bonnamour, N. Jaffrezic-Renault, H. Ben Ouada, J. Davenas, *J. Electroanal. Chem.* **2011**, *661*, 31–38.
[25] J.-M. Berquier, F. Creuzet, J.-M. Grimal, *Langmuir* **1996**, *12*, 597–598.
[26] A. Saftics, G. A. Prósz, B. Türk, B. Peter, S. Kurunczi, R. Horvath, *Sci. Rep.* **2018**, *8*, 11840.
[27] M. Rezayi, L. Y. Heng, A. Kassim, S. Ahmadzadeh, Y. Abdollahi, H. Jahangirian, *Sensors* **2012**, *12*, 8806–8814.
[28] L. Eddaif, L. Trif, J. Telegdi, O. Egyed, A. Shaban, *J. Therm. Anal. Calorim.* **2019**, *137*, 529–541.
[29] MicroVacuum, L. QCM-my-Quartz Crystal Microbalance with Impedance Measurement. Available at: http://www.owls-sensors.com/qcm-i-quartz-crystal-microbalance-with-impedance-measurement (2019).
[30] F. Ejeian, P. Etedali, H.-A. Mansouri-Tehrani, A. Soozanipour, Z.-X. Low, M. Asadnia, A. Taheri-Kafrani, A. Razmjou, *Biosens. Bioelectron.* **2018**, 118, 66–79.
[31] B. B. Narakathu, M. Z. Atashbar, B. E. Bejcek, *Biosens. Bioelectron.* **2010**, *26*, 923–928.
[32] P. Pulkkinen, J. Hassinen, R. Rasband, R. Tenhu, *RSC Adv.* **2014**, *4*, 13453.
[33] H. Kim, M. Lee, L. Mutihac, J. Vicens, J. S. Kim, *Chem. Soc. Rev.* **2012**, *41*, 1173–1190.
[34] L. Eddaif, A. Shaban, I. Szendro, *Electroanalysis* **2020**, *32*, 755–766.
[35] B. B. Adhikari, M. Gurung, H. Kawakita, K. Ohto, *Analyst* **2011**, *136*, 3758–3769.
[36] G. Horvat, L. Frkanec, N. Cindro, V. Tomišić, *Phys. Chem. Chem. Phys.* **2017**, *19*, 24316–24329.
[37] J. P. Santos, M. E. D. Zaniquelli, P. J. Dutton, *Colloids Surf. A* **2002**, *198*, 605–611.
[38] P. M. Marcos, S. Félix, J. R. Ascenso, M. A. P. Segurado, J. L. C. Pereira, P. Khazaeli-Parsa, V. Hubscher-Bruder, F. Arnaud-Neu, *New J. Chem.* **2004**, *28*, 748–755.
[39] H. Halouani, I. Dumazet-Bonnamour, M. Perrin, R. Lamartine, *J. Org. Chem.* **2004**, *69*, 6521–6527.
[40] S. J. S. Flora, V. Pachauri, *Int. J. Environ. Res. Public Health* **2010**, *7*, 2745–2788.
[41] F. Teme, M. Tabakci, *Talanta.* **2016**, *153*, 221–227.
[42] W. Sliwa, T. Girek, *J. Inclusion Phenom. Macrocyclic Chem.* **2010**, *66*, 15–41.

Received: July 12, 2020
Accepted: July 31, 2020
Published online on ■■, ■■

FULL PAPER

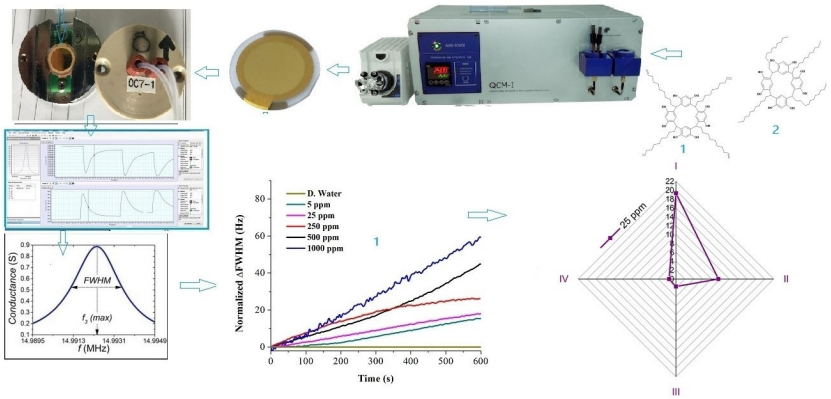

A. Shaban, L. Eddaif*